Turkish Journal of Physics

Volume 26 | Number 6 Article 7

1-1-2002

Characterization of the SnO_{2}/p Contact Resistance and SnO_{2} Properties in Operating a-Si:H p-i-n Solar Cells

RUHİ KAPLAN

BENGÜ KAPLAN

Follow this and additional works at: https://journals.tubitak.gov.tr/physics

Part of the Physics Commons

Recommended Citation

KAPLAN, RUHİ and KAPLAN, BENGÜ (2002) "Characterization of the SnO_{2}/p Contact Resistance and SnO_{2} Properties in Operating a-Si:H p-i-n Solar Cells," *Turkish Journal of Physics*: Vol. 26: No. 6, Article 7. Available at: https://journals.tubitak.gov.tr/physics/vol26/iss6/7

This Article is brought to you for free and open access by TÜBİTAK Academic Journals. It has been accepted for inclusion in Turkish Journal of Physics by an authorized editor of TÜBİTAK Academic Journals. For more information, please contact academic.publications@tubitak.gov.tr.

Turk J Phys
26 (2002) , 459 – 463.
© TÜBİTAK

Characterization of the SnO_2/p Contact Resistance and SnO_2 Properties in Operating a-Si:H p-i-n Solar Cells

Ruhi KAPLAN and Bengü KAPLAN
Department of Physics, University of Mersin, 33342 Mersin-TURKEY

Received 19.09.2001

Abstract

A method is presented to characterize the TCO/p contact and the TCO sheet resistance in a-Si TCO/p-i-n superstrate devices. It is extremely useful for understanding resistance losses in modulus and diagnosing how plasma processing influences the TCO layers. Analysis of 4-terminal dark J-V measurements as a function of temperature on devices with varying TCO geometry yields the TCO/p contact resistance $R_{TCO/p}$, its activation energy E_a or barrier height, and the TCO sheet resistance R_{SH} in an integrated device structure. The method is applied to devices fabricated on different brands of commercial SnO_2 substrates with different p-layers. Important new results are found. E_a for the SnO_2/p contact resistance are about 40-50 meV which is $< 2kT$, and therefore not a rectifying barrier. R_{SH} in one brand of SnO_2 has a benefical decrease of 60% after a-Si deposition while another brand is unaffected. The impact of R_{SH} or R_{TCO} losses on the FF (fill factor) are determined.

Key Words: TCO/p contact resistance, SnO_2 properties, a-Si:H p-i-n solar cells.

1. Introduction

Transparent conductive Oxides (TCO) have a crucial importance for the optical and electrical performance of amorphous silicon (a-Si) based solar cells. Minimizing the resistance between the p-layer and TCO of superstrate a-Si TCO/p-i-n solar cells, a critical issue for utilizing new TCO materials like ZnO, Zn-In-O and Zn-Sn-O and new p-layers like μc-SiC or μc-SiO. However, characterization of the TCO/p interface is difficult since it is in series with the dominant p-i-n junction.

This work builds upon the work presented in reference [1] where a new measurement configuration to characterize the SnO_2/p and SnO_2 sheet resistance was developed. That method required a complicated J-V testing configuration using the adjacent SnO_2 strip as a floating voltage probe, and required electrometers for their high input impedance. However, we have now developed an alternative method to obtain these parameters, using only one standard dark $J - V$ measurement per device. This method was applied to the samples used here. The only limitation is that it assumes a largely Ohmic contact between the SnO_2 and p-layer.

2. Experimental and Analysis

The sample matrix was 2 pieces of Asahi and 2 pieces of AFG SnO_2, each with p-i-n devices having different a-SiC p-layer recipes (S1 and S2), as shown in Table 1. The samples had laser scribed SnO_2, p-i-n deposition, and 0.25 cm^2 back contacts. Single junction a-Si p-i-n layers were deposited by PECVD at BP Solarex. Six devices were fabricated on each strip of SnO_2. Each SnO_2 strip of width W has a Ag-paste contact to the SnO_2 at one end, and 6 devices ($m = 1 - 6$) located in a row [1]. L is the distance along the TCO from the Ag contact to the m-th device, and L/W is the number of squares of TCO.

Table 1. Sample description, and final results of SnO_2 sheet resistance from Figure 5 and SnO_2/p activation energy and room temperature (fitted) contact resistance.

Sample	SnO_2	p-layer	R_{SH} (Ω/sq)	E_a of $R_{TCO/p}$ (meV)	$R_{TCO/p}$ $(\Omega - cm^2)$
A9251-3B	Asahi	S2	~ 10	42	0.44
A9251-4B	Asahi	S1	~ 11	39	0.83
A9256-3C	AFG	S2	~ 14	56	0.93
A9256-1B	AFG	S1	~ 14	53	0.64

The total series resistance of the m-th device (Equation 1) is the sum of the junction dynamic resistance R_J, the TCO/p contact resistance $R_{TCO/p}$, and the series resistance through the TCO R_{TCO}. R_{SH} is the sheet resistance of the TCO in Ω/sq. Thus we write

$$R = dV/dJ = R_J + R_{TCO/p} + R_{TCO} \tag{1}$$

$$R_{TCO} = R_{SH} \times (L/W) \tag{2}$$

$$R_J = (AkT/q)/J \tag{3}$$

$$R_S = R_{TCO/p} + R_{TCO}. \tag{4}$$

As L increases, the series resistance of the TCO between the device and its SnO_2 contact increases. Plotting R_S versus L/W will have an intercept of the series resistance R_S and slope AkT/q. Plotting R_S versus L/W will have an intercept of $R_{TCO/p}$ and a slope of R_{SH}.

3. Results

Figure 1 shows the dark J-V curves at 296 K of 5 devices on A9256-3C (AFG SnO_2, S2 p-layer) measured using the same SnO_2 contact at one end of the strip. The series resistance R_S increases as the distance L between the device and the SnO_2 contact increases. The SnO_2 strip width W was 0.80 cm. The dark J-V behavior at various temperatures for L/W=1.65 of the same device is shown in Figure 2. As the temperature increases, the slopes (dV/dJ) of the forward bias dark characteristics move to lower voltages.

Figure 3 shows the derivative dV/dJ of the data given in Figure 1 plotted versus $1/J$. The data almost forms a series of parallel lines with increasing intercept. The intercept is the series resistance R_S and it increases steadily from about 2 to 18 $\Omega\cdot$ cm^2 as L/W increases. R_S is the sum of the SnO_2 sheet resistance R_{SH}, which increases linearly with L/W, and the contact resistance, which should be independent of L/W. The slope of the data is AkT/q, indicating A values of 1.6-1.8 at room temperature, 296 K. (The 3 other samples actually had A values typically of 1.8-2.0).

In Figure 4, we have plotted the intercepts R_S against L/W. Data is shown for 13 temperatures (from 223 to 393 K) that we measured. The fit is excellent, and the intercept steadily decreases while the slope increases slightly ($\sim$ 10%). We attribute the intercept to the SnO_2/p contact (R_{SnO_2}/p) and the slope to the SnO_2 resistance. R_{SnO_2}/p is actually the sum of all fixed resistances in the device, but we feel we have ruled out any significant contribution from the back contact and the Ag paste contact to the SnO_2. At the highest temperatures, we typically found intercepts of less than 0.3 $\Omega\cdot$ cm^2, indicating that any residual resistances in the circuit were negligible.

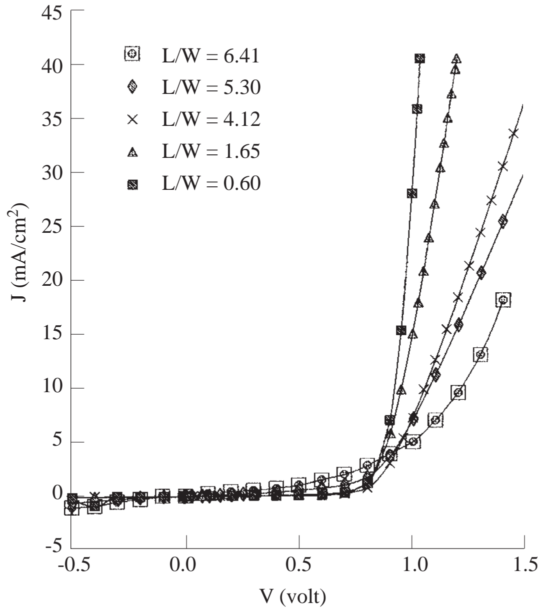

Figure 1. J-V in dark at 296 K of five devices (with various L/W) along a SnO_2 strip on A9256-3C.

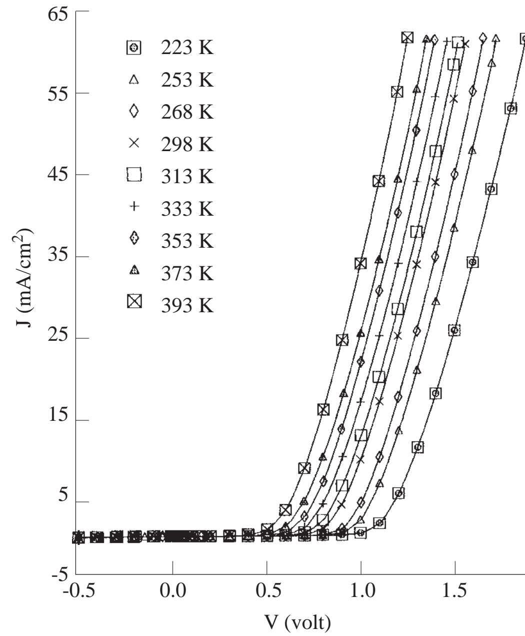

Figure 2. J-V in dark at various temperatures for A9256-3C devices on a strip of AFG SnO_2. (L/W = 1.65).

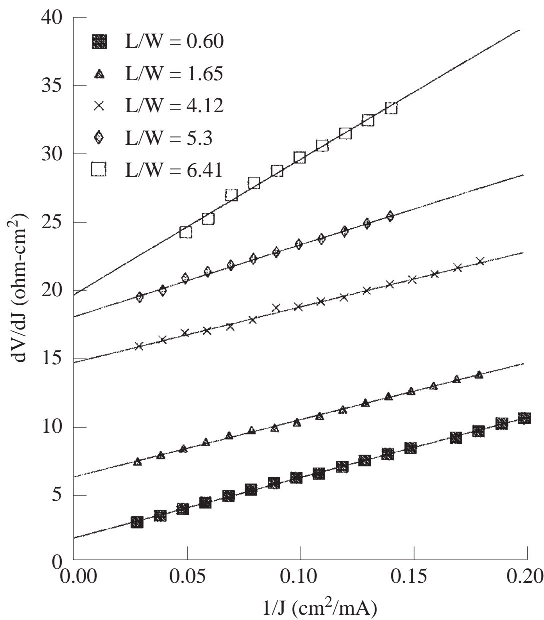

Figure 3. dV/dJ vs $1/J$ for same 5 J-V curves of Figure 1.

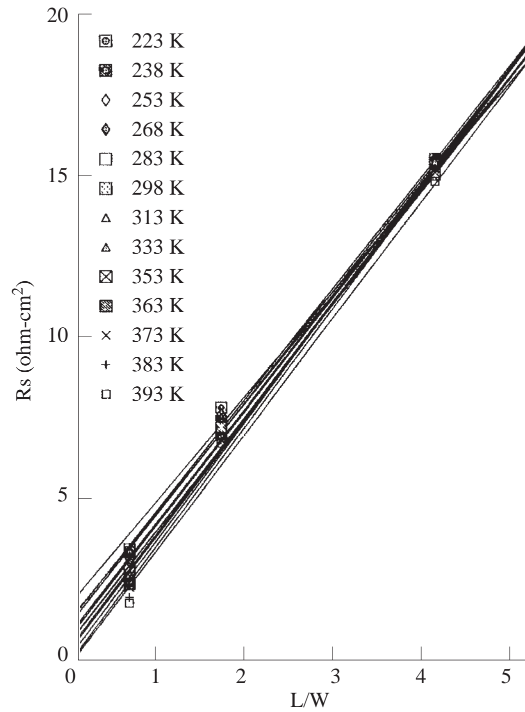

Figure 4. R_S from intercept of dV/dJ curves at 13 temperatures vs L/W, and fit. (Sample, A9256-3C).

Figure 5 shows the general temperature independence of R_{SH}, obtained from the slopes of R_S versus L/W at each temperature. This is as expected for a degenerate semiconductor. Over the range from 223 to 393 K, note that the two AFG pieces have $R_{SH} \sim 13-14\ \Omega/sq$ while the two Asahi pieces have $\sim 10 - 11$ Ω/sq. Thus, we conclude both p-layers had a similar effect on their SnO_2. The bare AFG which we received

along with these samples had R_{SH} of 14 - 15 while the Asahi had 16-17 Ω/sq. Thus, the R_{SH} for AFG is not affected by the device processing while R_{SH} for Asahi SnO_2 is reduced by $\sim 60\%$. This is very consistent with the H_2 plasma study which showed the sheet resistance of Asahi decreased a similar amount, with either H_2 plasma or $\mu c-Si$ growth, due to increase in mobility [2, 3, 4]. AFG SnO_2 was unaffected by either process. This is further confirmation that Asahi SnO_2, with its lover carrier density, is easily improved during standard processing while AFG SnO_2 is immune to improvement, at least under the conditions explored so far.

Figure 6 shows the temperature dependence of the SnO_2/p resistance. This is really the goal of the research. The data is somewhat noisy, perhaps related to the fact it is the result of 3-fold reduction in data (3 iteration of fitting results of analysis of experimental data). Extreme outlying points are not shown. Accepting the moderately good fit, the activation energies calculated from the exponential terms, and the fitted value at 296 K, are shown in Table 1. The 2 Asahi pieces had $E_a \sim 40$ meV while the two AFG had ~ 54 meV. It is not meaningful to speculate further about differences between S1 and S2 p-layers due to the uncertainty in fitting. Note that the activation energy of the SnO_2 was ~ 0 while that of the p-layer is $\sim 0.3 - 0.4$ eV. Thus, the E_a value in Table 1 which we attribute to the contact is quite different from that of either material forming the contact. The expected value of R_{SnO_2}/p at room temperature is in the range of 0.5 to 1 $\Omega\cdot$ cm^2. Similar results were also obtained in ZnO/p contact [5].

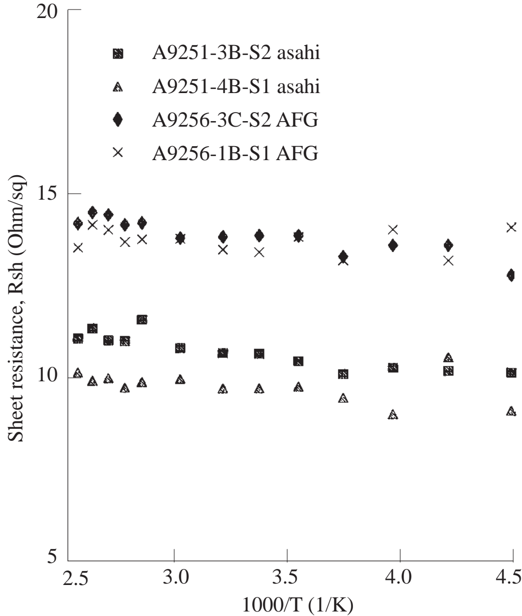

Figure 5. SnO_2 sheet resistance (R_{SH}) vs $1/T$ (from dark dV/dJ) for all 4 samples. Initial R_{SH}= 17 Ω/sq (Asahi) and 14 Ω/sq (AFG).

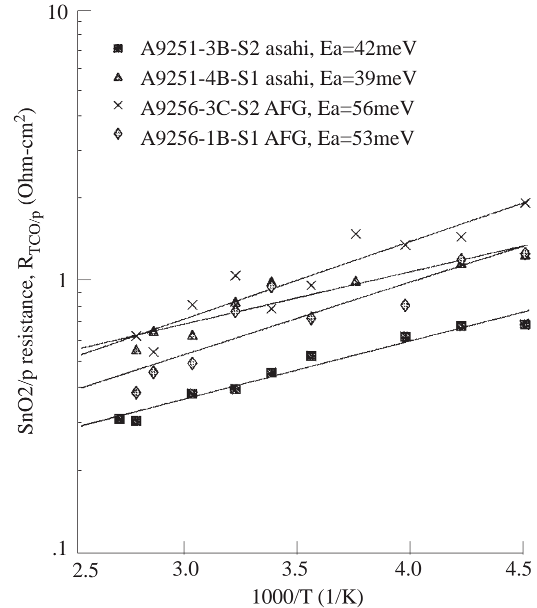

Figure 6. SnO_2/p contact resistance ($R_{TCO/p}$) vs $1/T$ (from intercept of R_S vs L/W) for all 4 samples, including fit.

We measured the J-V performance under AM1.5 illumination after all J-V-T measurements were completed. Results are in Table 2. The largest difference between the samples is that S1 p-layers have noticable higher J_{SC}. There was no difference in V_{OC} or FF, which might have related to the parameters in Table 1.

Table 2. Measured $J-V$ parameters after $J-V-T$ testing and 20 minute anneal at 150^oC. Results from best cell of 3 tested with minimum L/W (highest FF). R_{OC} is the resistance (dV/dJ) at V_{OC}.

Sample	$V_{OC}(V)$	$J_{SC}(mA/cm^2)$	$FF(\%)$	$Eff.(\%)$	$R_{OC}(\Omega-cm^2)$
A9251-3B	0.88	14.2	68.3	8.6	6.5
A9251-4B	0.88	15.8	67.6	9.4	7.8
A9256-3C	0.88	12.6	68.7	7.7	7.2
A9256-1B	0.89	15.4	68.4	9.3	7.8

4. Conclusions

We have developed a newer and easier method to obtain SnO_2 parameters in a device configuration. We have shown that the SnO_2/p contact has a barrier of 40-55 meV indicating an Ohmic contact. $R_{TCO/p}$ was 0.5 - 1 $\Omega\cdot$ cm^2 for 1 set of p-layer conditions on either AFG or Asahi SnO_2. This corresponds to a negligible $\sim 0.05-0.1\%$ loss in efficiency. The sheet resistance of the Asahi brand SnO_2 decreased $\sim$ 60% with a-Si processing. This is consistent with reports of others. This new technique can be useful in evaluating factors which affect the TCO/p contact resistance, such use of new TCO materials or p-layer processing.

Acknowledgments

We would like to thank Dr. S. Hegedus for valuable discussions. Dr. R. Kaplan acknowledges the Fulbright Scholars Program which funded in part this work at the Institute of Energy Conversion, University of Delaware.

References

[1] S. Hegedus, M.Gibson, G. Ganguly, R. Arya, *MRS Symp Proc.* **557**, 1999, p.737.

[2] L. Yang, M. Bennett, L. Chen, K. Jansen, J. Kessler, Y. Li, J. Newton, K. Rajan, F. Willing, R. Arya, D. Carlson, *Mat.Res. Soc. Symp. Proc.* **426**, 1996, p.3.

[3] K. Sato, Y. Gotoh, Y. Hayashi, H. Nishimura, Proc. 21st IEEE PVSC, 1990, p.1584.

[4] M. Kubon, N. Shultz, M. Kolter, C. Beneking, H. Wagner, Proc. 12th Euro, PVSC, 1994, p.1268.

[5] S. Hegedus, R. Kaplan, G. Ganguly, G.S. Wood, Proc. 28th IEEE Photovoltaic Specialists Conference, 2000, pp. 728-731.